Oxidative Addition of the C−S Bond of Thiophene to the $(C_5Me_5)Rh(PMe_3)$ Fragment: A Theoretical Study Revisited

Tülay A. Ateşin and William D. Jones*

Department of Chemistry, University of Rochester, Rochester, New York 14627

Received September 7, 2007

Density functional theory (DFT) calculations on the C−S bond activation reaction of thiophene with the $[(C_5Me_5)Rh(PMe_3)]$ fragment have been reinvestigated, giving two new isomeric C−S bond activation transition states, in which the coordinated thiophene molecule tilts toward either the C_5Me_5 ligand or the PMe_3 ligand. Through intrinsic reaction coordinate (IRC) calculations, these transition states were found to connect the oxidative addition product with two isomeric η^2-C,S coordinated intermediates. These latter intermediates in turn connected to two isomeric η^1-S and η^2-C,C coordinated species. The energetics and mechanistic details are described.

Introduction

Fundamental studies on hydrodesulfurization (HDS),[1] which is the general process for removal of sulfur from petroleum, maintain their importance due to the more stringent new regulations on the sulfur content allowed in petroleum.[2] Optimization of the HDS catalyst could follow from a better understanding of the reaction mechanism of this heterogeneous process.[3] Since the breaking of C−S bonds is a necessary step in HDS, the insertion of metal complexes into the C−S bond of thiophene is widely studied in the homogeneous HDS models.[4]

One such metal complex shown to insert into a variety of thiophene carbon−sulfur bonds is the reactive 16 electron metal fragment $[(C_5Me_5)Rh(PMe_3)]$.[5] In this experimentally well-characterized model system, the thermal reaction of the $[(C_5Me_5)Rh(PMe_3)]$ fragment with thiophene yields only the C−S bond activation product **1**, whose planar structure and numbering scheme are shown in Figure 1.[6]

Density functional theory (DFT) using B3LYP was first used to study the reaction of thiophene and the $[(C_5Me_5)Rh(PMe_3)]$ fragment by Sargent to discern the key features of the C−S bond activation mechanism and to determine the structures and relative energetics of the reactive intermediates and transition states which were difficult or impossible to determine experimentally.[7] In this study, the structure of the transition state connecting the η^1-S coordinated intermediate with the C−S bond-activated product, $\mathbf{TS_{C-S}}$,[8] was located by using the quadratic synchronous transit (QST) calculations, which require the reactant and product structures as input. However, the structure reported for the C−S cleavage transition state $\mathbf{TS_{C-S}}$

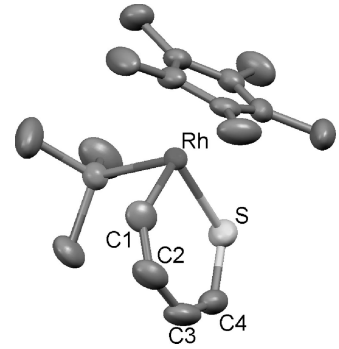

Figure 1. POV-RAY drawing of the X-ray structure of **1** showing numbering scheme. Ellipsoids are shown at the 50% probability level.

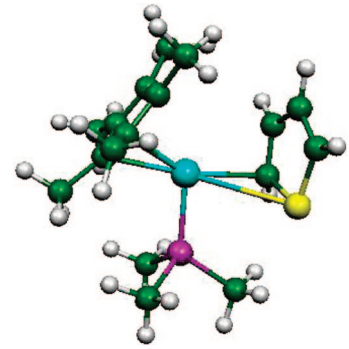

Figure 2. Optimized structure of the "transition state" for C−S bond cleavage of thiophene by [Cp*Rh(PMe$_3$)] reported by Sargent (ref 7), $\mathbf{TS_{C-S}}$: $d_{S-C\alpha} = 1.884$ Å; $d_{Rh-S} = 3.206$ Å; $d_{Rh-C\alpha} = 2.196$ Å; $d_{Rh-C\beta} = 2.716$ Å.

* Address correspondence to this author. E-mail: jones@chem.rochester.edu.

(1) Schuman, S. C.; Shalit, H. *Catal. Rev.* **1970**, *4*, 245.

(2) Fed. Regist. 2000, *65*, 6697−6746. From the Federal Register Online via GPO Access [wais.access.gpo.gov].

(3) Sanchez-Delgado, R. A. *Organometallic Modelling of the Hydrodesulphurization and Hydronitrogenation Reactions*; Kluwer Academic Publishers: Dordrecht, 2002; p 1.

(4) (a) Sanchez-Delgado, R. A. *J. Mol. Chem.* **1994**, *86*, 287. (b) Bianchini, C.; Meli, A. *J. Chem. Soc., Dalton Trans.* **1996**, 801. (c) Bianchini, C.; Meli, A. *Acc. Chem. Res.* **1998**, *31*, 109. (d) Bianchini, C.; Meli, A. *Transition Metal Sulphides. Chemistry and Catalysis*; Weber, T., Prins, R., van Santen, R. A., Eds.; NATO ASI Series; Kluwer: Dordrecht, 1998; Vol. 60, pp 129−154. (e) Garcia, J. J.; Mann, B. E.; Adams, H.; Bailey, N. A.; Maitlis, P. M. *J. Am. Chem. Soc.* **1995**, *117*, 2179. (f) Garcia, J. J.; Maitlis, P. M. *J. Am. Chem. Soc.* **1993**, *115*, 12200.

(5) (a) Jones, W. D.; Dong, L. *J. Am. Chem. Soc.* **1991**, *113*, 559. (b) Dong, L.; Duckett, S. B.; Ohman, K. F.; Jones, W. D. *J. Am. Chem. Soc.* **1992**, *114*, 151.

(6) Blonski, C.; Myers, A. W.; Palmer, M.; Harris, S.; Jones, W. D. *Organometallics* **1997**, *16*, 3819.

(7) Sargent, A. L.; Titus, E. P. *Organometallics* **1998**, *17*, 65.

(8) In labeling compounds, the prefix **S** or **TS** is used to denote a calculated structure.

10.1021/om700899n CCC: $40.75
Publication on Web 07/17/2008

Table 1. Gas-Phase-Optimized Structures (Distances in Å) and Relative Gibbs Free Energies (ΔG, kcal mol^{-1}) of Stationary Points on the [(C_5Me_5)Rh(PMe_3)] Fragment + Thiophene Potential Energy Surface (Atom Numbering Is As Shown in Figure 1)

	Rh−S	Rh−C1	Rh−C2	S−C1	C1−C2	C2−C3	C3−C4	C4−S	Rh−P	ΔG [a]
S1	2.308	3.554	4.544	1.750	1.363	1.438	1.363	1.755	2.272	−20.3
S1′	2.301	3.624	4.672	1.753	1.365	1.437	1.365	1.753	2.277	−18.9
TS14	2.457	2.745	3.671	1.763	1.382	1.421	1.375	1.749	2.269	−13.1
TS1′4′	2.430	2.693	3.725	1.764	1.385	1.420	1.375	1.751	2.280	−12.9
S2	3.428	2.124	2.172	1.812	1.451	1.461	1.352	1.765	2.406	−25.5
S2′	3.543	2.117	2.179	1.812	1.447	1.458	1.352	1.765	2.318	−23.6
TS24	3.214	2.261	2.720	1.786	1.408	1.417	1.375	1.727	2.272	−5.3
TS2′4′	3.146	2.294	2.987	1.771	1.400	1.415	1.380	1.723	2.263	−5.9
S3	2.382	2.029	3.091	3.211	1.351	1.454	1.354	1.750	2.299	−35.5
TS34	2.379	2.109	3.150	2.138	1.394	1.416	1.375	1.740	2.322	−12.4
TS34′	2.370	2.102	3.241	2.152	1.391	1.415	1.376	1.737	2.032	−11.0
S4	2.469	2.222	3.213	1.822	1.423	1.398	1.391	1.734	2.295	−15.3
S4′	2.464	2.228	3.326	1.817	1.421	1.398	1.392	1.733	2.301	−14.4
TS_{C-S} [b]	3.206	2.196	2.716	1.884	1.437	1.443	1.399	1.803	2.369	−11.1[c]

[a] Sum of electronic and thermal free energies. [b] Transition state reported in ref 7 to form **3**. [c] Electronic energy rather than free energy is listed.

showed a very long Rh−S distance (3.206 Å) and almost no lengthening of the C−S bond (1.884 Å), inconsistent with a transition-state structure for C−S cleavage. In addition, there was a close proximity of the distal carbons on thiophene with the methyl groups of the C_5Me_5 group, leading to reduced bonding of the C_5Me_5 group (Figure 2). C−H activation of the α-thienyl C−H bonds was also investigated in this study by Sargent, as observed experimentally at low temperature.

In a separate study done by Lledós on the same system, the hybrid quantum mechanics/molecular mechanics (QM/MM) method IMOMM was applied to each reaction step to quantify and separate the effect of methyl substituents in both C_5Me_5 and PMe_3 ligands into steric and electronic contributions.[9] This study showed that substitution at the 3 and 4 positions of thiophene have a more significant steric effect on the C−S bond cleavage barrier compared to substitution at the 2 and 5 positions, contrary to previously reported experimental studies[5] which demonstrated that the insertion reaction with 2-methyl thiophene gave one product, whereas 3-methyl thiophene gave two insertion products in a 1:1 ratio.

The reactions of substituted thiophenes with the [(C_5Me_5)Rh(PMe_3)] fragment have been studied experimentally in our laboratory.[10] To be able to interpret the observed experimental selectivity in these bond cleavage reactions, we decided to conduct DFT calculations taking these prior theoretical studies with thiophene as a starting point while adding substituents to the transition-state structure found in the literature. However, intrinsic reaction coordinate (IRC) calculations starting from the modified transition states did not lead to the formation of the C−S bond cleavage products.[11] Therefore, we re-examined the published calculations to locate the correct transition state for the C−S bond cleavage of thiophene. Our results, described herein, show that the transition-state geometry reported in the literature (species **5** in ref 7) *is not the transition state for C−S cleavage* but rather for another process interconverting coordination isomers with an intact thiophene ring. We have located the correct transition state and find that there are two possible orientations for binding the thiophene to the metal prior to C−S cleavage. The barriers to the C−S cleavage product are remarkably similar from these species.

(9) Maresca, O.; Maseras, F.; Lledós, A. *New J. Chem.* **2004**, *28*, 625.
(10) Myers, A. Ph. D. Thesis, University of Rochester, Rochester, NY, 1995. Myers, A. W.; Dong, L.; Ateşin, T. A.; Skugrud, R.; Jones, W. D. Inorg. Chim. Acta, in press.
(11) Ateşin, T. A.; Jones, W. D. submitted to *Inorg. Chem.*

Results and Discussion

As reported earlier, the thermal reaction of the fragment [$C_5Me_5Rh(PMe_3)$] with thiophene leads to the formation of the C−S insertion product as the only stable product.[5] In our reexamination of this system using DFT/B3LYP calculations, the fully methylated system was employed in the model, as these steric interactions have been shown to be of importance.[9] The optimizations of all of the ground-state and the transition-state structures were done in the gas phase. Two parallel series of compounds, one set with the thiophene synclinal toward the C_5Me_5 ligand and the other with the thiophene anticlinal toward the C_5Me_5 ligand (i.e., leaning toward the PMe_3 ligand), were calculated to account for all the possible structures in this reaction. The relative energies of the optimized structures were calculated with respect to the free fragments as the zero of energy. Selected structural parameters and the relative free energies are given in Table 1, while the optimized structures are shown in Schemes 1 (synclinal) and 2 (anticlinal). Several, but not all, of these synclinal species were located in the earlier computational study.[7] With the exception of one transition state (**TS24**), the synclinal isomers are found to be slightly more stable than the anticlinal isomers (by ∼1 kcal/mol).

Location of a New η^2-C,S-Thiophene Intermediate. While searching for the transition state for C−S cleavage, a stable η^2-C,S-thiophene complex **S4** was discovered, *which is not one of the intermediates proposed in the prior literature*. This species was located using relaxed potential energy surface scans,[12] starting with either the optimized structure of the η^1-S coordinated intermediate reported in the literature[7] (**S1**) and pulling the α-carbon atom closer to the rhodium metal or starting with the optimized structure of the η^2-C,C coordinated intermediate (**S2**) and pulling the sulfur atom closer to the rhodium metal. Transition states with synclinal orientations of the thiophene were located connecting species **S1** and **S2** with **S4** (**TS14** and **TS24**, respectively), this motion constituting a migration of the metal around the π-system of the thiophene ring as verified by intrinsic reaction coordinate (IRC) calculations.

An anticlinal analogue of the η^2-C,S-thiophene complex **S4′**, as well as anticlinal analogues of the S-bound (**S1′**) and η^2-C,C-bound (**S2′**) thiophene complexes, was similarly identified, as were transition states joining species **S1′** and **S2′** with **S4′** (**TS1′4′** and **TS2′4′**, respectively) (see the Supporting Information for details). Synclinal **S1** is found to be 1.4 kcal mol^{-1} more stable than anticlinal **S1′**, and as interconversion of **S1**

(12) Foresman, J. B.; Frisch, A. E. *Exploring Chemistry with Electronic Structure Methods*; Gaussian, Inc.: Pittsburgh, 1993; pp 171−4.

Scheme 1. Optimized Structures of Stationary Points on the [(C_5Me_5)Rh(PMe_3)] + Thiophene Potential Energy Surface: Synclinal Isomers

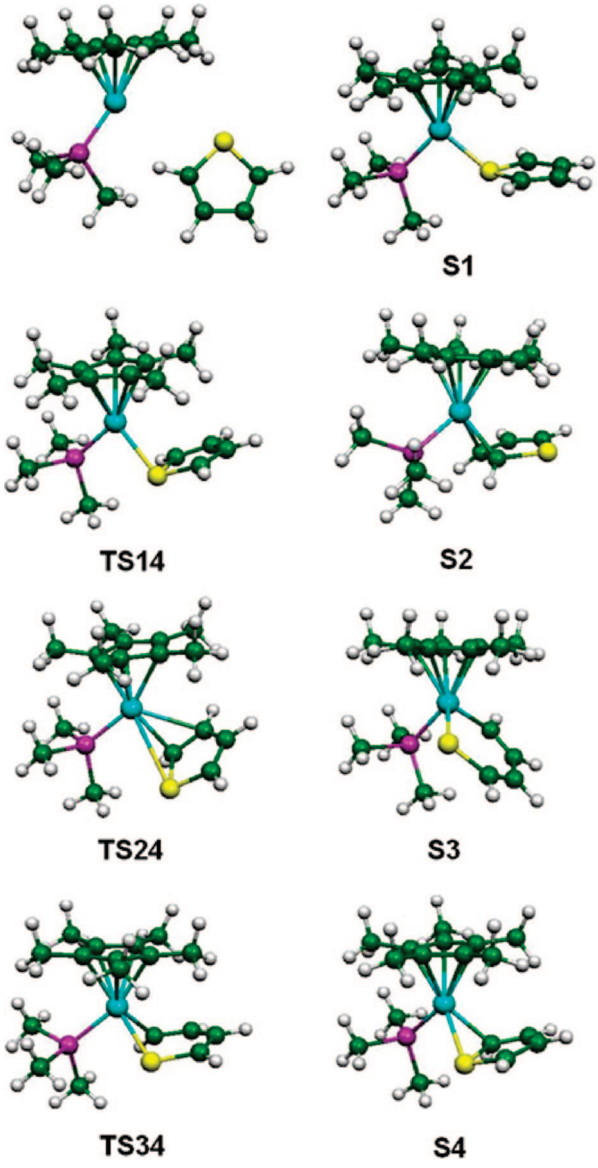

Scheme 2. Optimized Structures of Stationary Points on the [(C_5Me_5)Rh(PMe_3)] + Thiophene Potential Energy Surface: Anticlinal Isomers

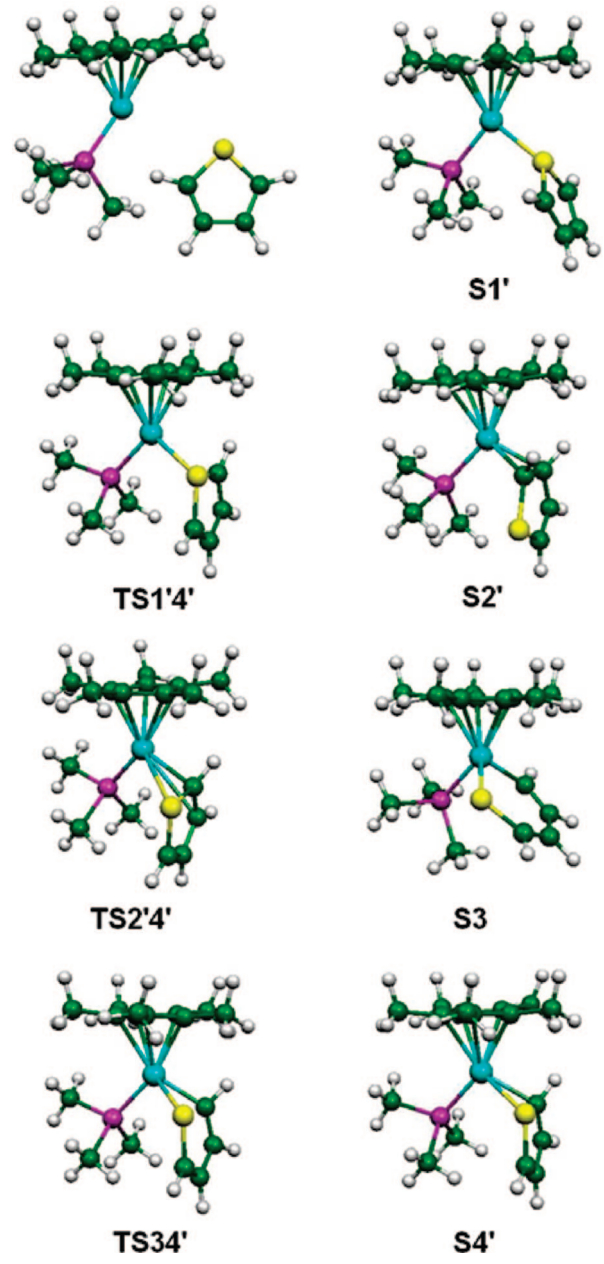

and **S1′** is facile (see the Supporting Information, Figure SI-8), **S1** should be the dominant S-bound species. Likewise, synclinal **S2** is also calculated to be more stable than anticlinal **S2′** by 1.9 kcal/mol, and as Rh−olefin bond rotation is rapid (6 kcal/mol in $CpRh(C_2H_4)_2$[13]), **S2** should be the dominant η^2-C,C-bound species. Synclinal rotamer **S4** is also more stable than rotamer **S4′** (by 0.9 kcal/mol). Consequently, synclinal rotamers dominate as the preferred thiophene-bound species.

The only case where an anticlinal rotamer is more stable is in the case of **TS2′4′**, although the energy difference in all cases is less than 2 kcal/mol. In **TS24**, as the thiophene molecule tilts toward the C_5Me_5 ligand to bring the sulfur atom closer to the rhodium metal, the distance between rhodium and the centroid of the C_5Me_5 ligand increases dramatically (to 2.082 Å), which causes considerable destabilization in this transition state. In fact, this transition state is the one identified by Sargent as the "C−S cleavage" transition state **5**,[7] which was located from the η^1-coordinated intermediate **S1** and the C−S addition product **S3** by the QST3 method. (See the Supporting Information for an overlay of these two structures).

Location of the Transition State for C−S Bond Cleavage. The transition state for C−S cleavage, **TS34**, was obtained starting from **S4** and moving apart the C−S atoms in a relaxed potential energy scan (Figure 3). IRC calculations showed that this transition state was directly connected to the oxidative addition product **S3** in one direction and the stable η^2-C,S adduct **S4** in the other direction. Interestingly, if the optimized structure of the oxidative addition product **S3** was used as the starting point for the C−S bond cleavage transition-state calculations, and the C1−S distance decreased using a relaxed potential energy scan, a different transition state for the C−S bond cleavage (**TS34′**) was located. This transition state shows an *anticlinal* geometry of the thiophene ring in which it is oriented away from the C_5Me_5 ring, even though the SC_4 plane was initially tilted slightly (by 6°) toward the C_5Me_5 ring in **S3**!

Optimization of **TS34′** as a transition state, and connection to **S3** and **S4′** via IRC calculations, shows this pathway to be

(13) Cramer, R. *J. Am. Chem. Soc.* **1964**, *86*, 217.

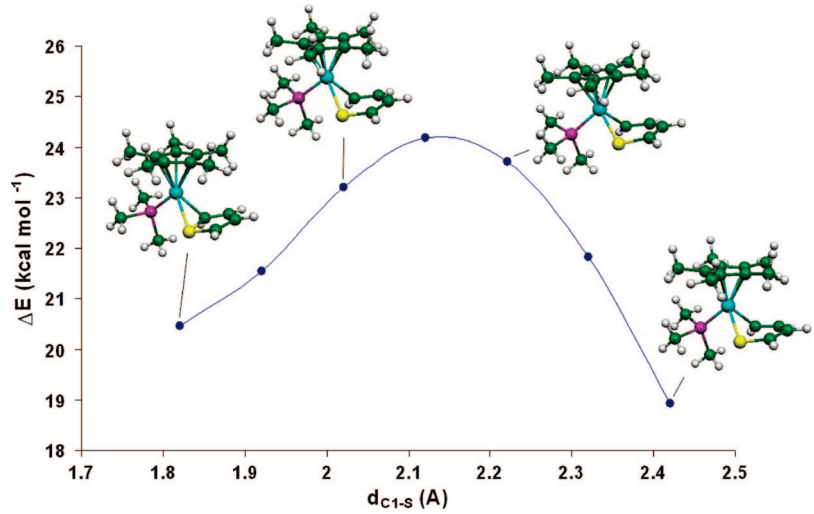

Figure 3. Locating the C−S cleavage transition state, **TS34**, by stepwise lengthening of the C−S distance in **S4**.

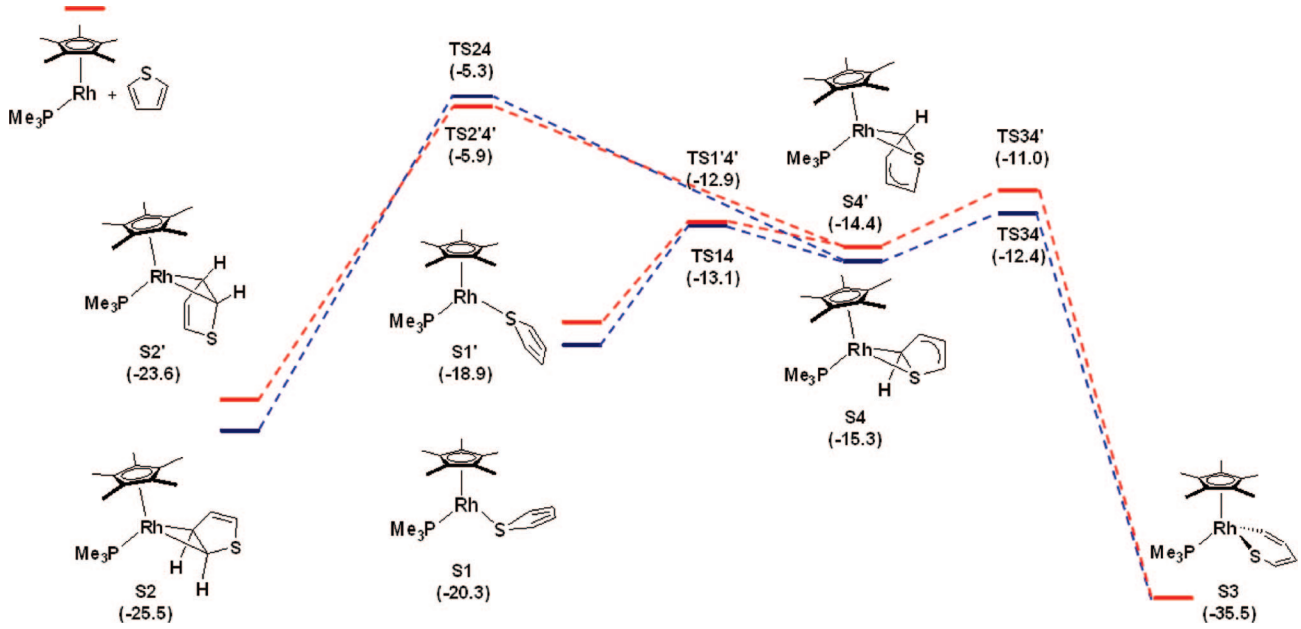

Figure 4. Energetics of the C−S bond activation of thiophene by [(C_5Me_5)Rh(PMe_3)] fragment (free energies in kcal/mol at 298 K) relative to the total energies of fragments ([(C_5Me_5)Rh(PMe_3)] + thiophene).

1.4 kcal/mol higher in energy than the synclinal pathway via **TS34**. Consequently, in light of the facile interconversion of **S2/S2′** and **S1/S1′** *the minimum energy pathway for C−S bond cleavage occurs via synclinal complex* **S4** *and synclinal transition state* **S34**. Selected geometrical parameters and the relative energies with respect to the total free energy of the fragments of the optimized transition-state structures **TS34′** and **TS34** (as well as $\mathbf{TS_{C-S}}$ from ref 7) are indicated in Table 1. The interatomic distances in **TS34** and **TS34′** are very similar to each other, while significantly different from those in $\mathbf{TS_{C-S}}$, as the latter turns out not to be the transition state for bond cleavage. In the true C−S cleavage transition state, the Rh−C1 and Rh−S bond lengths (2.109 and 2.379 Å, respectively) are within 0.01 Å of their final values in insertion product **S3**, and there is considerable elongation of the S−C1 bond (0.4 Å). Thus, the formation of the Rh−C1 and Rh−S bonds is much more advanced than the breaking of the S−C1 bond in the transition state for the C−S cleavage. Contrary to what has been reported in the literature, we find that the C−S bond scission and Rh−C and Rh−S bond-formation steps involved in the C−S bond activation reaction of thiophene with the [(C_5Me_5)Rh(PMe_3)] fragment are not concerted.

The energetics of the C−S bond activation of thiophene by the [(C_5Me_5)Rh(PMe_3)] fragment relative to the total energies of the separate fragments are shown in Figure 4. All of the optimized synclinal structures in which the bound thiophene molecule is tilted toward the C_5Me_5 ligand are shown to be more stable than their anticlinal isomers except in **TS24**, although the energy difference in all cases is less than 2 kcal/mol. Although the η^1-coordinated intermediates **S1** and **S1′** are significantly higher in energy than the η^2 coordinated isomers (**S2** and **S2′**), the transition states from the former to the η^2-C,S species are considerably lower in energy than from the latter. This might be due to the η^3-like coordination required for migration of the metal from the C=C double bond to the C−S σ bond in the transition states **TS24** and **TS2′4′**, compared to the simple approach of C1 to rhodium in converting the S-bound complex to the η^2-C,S complex. Initial coordination of the metal to thiophene can occur at either the sulfur or the C−C double bond—calculations cannot tell us which is kinetically preferred.

Binding to sulfur leads to C−S cleavage via synclinal rotamers, but binding to the C−C double bond proceeds to products via an anticlinal isomer to avoid interactions with the C_5Me_5 ring. Regardless of how the thiophene initially binds, it is remarkable how similar the barriers are throughout the reaction.

Conclusions

These results modify the earlier proposed mechanism in which η^1-S coordination leads directly to C−S bond activation. In fact, both η^1-S coordination and η^2-C,C coordination lead to an additional stable η^2-C,S intermediate that immediately precedes C−S cleavage, with a synclinal geometry being slightly favored over an anticlinal geometry. It is also interesting to note that the transition state for C−S cleavage discovered here with $[C_5Me_5Rh(PMe_3)]$ is similar to the one found for [(dippe)Pt][14] in two ways. First, an η^2-C,S-thiophene intermediate was found to precede C−S cleavage, and second, formation of the metal−sulfur and metal−carbon bonds is pretty much complete (within 4% of final distances) although there is more C−S bond breaking with Rh (d_{C-S} = 2.14 Å) than with Pt (d_{C-S} = 2.041 Å). This may be a hallmark of these compounds that cleave C−S bonds via oxidative addition.

Experimental Section

Computational Methods. When available, known experimental structures for the complexes were used as the starting points for the calculations, although as noted above this does not necessarily locate the minimum energy transition state for a reaction step. No simplifications were done by replacing the C_5Me_5 ligand with C_5H_5 and the PMe_3 ligand with PH_3, due to the importance of steric and electronic contributions of methyl substituents in both C_5Me_5 and PMe_3 ligands. The gas-phase structures were fully optimized in redundant internal coordinates,[15] with density-functional theory (DFT) and a wave function incorporating Becke's three-parameter hybrid functional (B3),[16] along with the Lee−Yang−Parr correlation functional (LYP).[17] All calculations were performed using the Gaussian03[18] package. The Rh, P, and S atoms were represented with the effective core pseudopotentials of the Stuttgart group and the associated basis sets improved with a set of f-polarization functions for the transition metal (α = 1.350, Rh)[19] and a set of d-polarization functions for the main group elements (α = 0.387, P; α = 0.503, S).[20] The atoms in the thiophenic ring and those directly bound to the metal were represented with 6-31G(d,p)[21] basis sets. As the size of the system involved in this processes still poses a challenge to current computational resources, the remaining atoms were represented with a smaller basis set (6-31G).[22] The geometry optimizations were performed without any symmetry constraints. The initial guess for the transition-state structures obtained from the relaxed potential energy surface scans[12] were optimized to a first-order saddle point. The local minima and the transition states were checked by frequency calculations. For each transition-state structure, the intrinsic reaction coordinate (IRC) routes were calculated in both directions toward the corresponding minima.[12] For some of the transition states, the IRC calculations failed to reach the energy minima on the potential energy surface in reasonable times due to the flatness of the surface near the transition state (for **TS34** and **TS34′**, reverse IRCs stopped after only 4 points out of 10 were optimized); therefore, in those cases geometry optimizations were carried out as a continuation of the IRC path. The energies used in the relaxed potential energy surface scan figures are electronic energies without any ZPE corrections, while those in Table 1 are the sum of electronic and thermal free energies calculated at 298.15 K and 1 atm.

Acknowledgment. We acknowledge the NSF for financial support (CHE-0414325 and CHE-0717040). We also thank Ting Li for calculations pertaining to the estimate of the barrier to Rh−S rotation in **1**.

Supporting Information Available: Comparison of gas-phase optimized structure and X-ray crystal structure of the C−S bond activation product of thiophene by the $[(C_5Me_5)Rh(PMe_3)]$ fragment. Computational methodology used in locating of transition states **TS14**, **TS24**, **TS34**, and **TS34′** and for connecting **S4′** to **S1′** and **S2′** via **TS1′4′** and **TS2′4′**. A figure showing an overlay of transition state **TS24** and transition state **5** from ref 7. A figure showing the barrier to Rh−S rotation in **S1**. Optimized geometries of the ground-state structures (**S1**, **S1′**, **S2**, **S2′**, **S3**, **S4**, and **S4′**) and transition-state structures (**TS14**, **TS1′4′**, **TS24**, **TS2′4′**, **TS34**, and **TS34′**), as well as the fragments in the gas phase. Sample input files for geometry optimizations. Animated movie files of the transition states are also available online. This material is available free of charge via the Internet at http://pubs.acs.org.

OM700899N

(14) Ateşin, T. A.; Jones, W. D. *Organometallics* **2008**, *27*, 53.
(15) Peng, C.; Ayala, P. Y.; Schlegel, H. B.; Frisch, M. J. *J. Comput. Chem.* **1996**, *17*, 49.
(16) Becke, A. D. *J. Chem. Phys.* **1993**, *98*, 5648.
(17) Lee, C.; Yang, W.; Parr, R. G. *Phys. Rev. B* **1988**, *37*, 785.
(18) Frisch, M. J.; Trucks, G. W.; Schlegel, H. B.; Scuseria, G. E.; Robb, M. A.; Cheeseman, J. R.; Montgomery, J. A., Jr.; Vreven, T.; Kudin, K. N.; Burant, J. C.; Millam, J. M.; Iyengar, S. S.; Tomasi, J.; Barone, V.; Mennucci, B.; Cossi, M.; Scalmani, G.; Rega, N.; Petersson, G. A.; Nakatsuji, H.; Hada, M.; Ehara, M.; Toyota, K.; Fukuda, R.; Hasegawa, J.; Ishida, M.; Nakajima, T.; Honda, Y.; Kitao, O.; Nakai, H.; Klene, M.; Li, X.; Knox, J. E.; Hratchian, H. P.; Cross, J. B.; Bakken, V.; Adamo, C.; Jaramillo, J.; Gomperts, R.; Stratmann, R. E.; Yazyev, O.; Austin, A. J.; Cammi, R.; Pomelli, C.; Ochterski, J. W.; Ayala, P. Y.; Morokuma, K.; Voth, G. A.; Salvador, P.; Dannenberg, J. J.; Zakrzewski, V. G.; Dapprich, S.; Daniels, A. D.; Strain, M. C.; Farkas, O.; Malick, D. K.; Rabuck, A. D.; Raghavachari, K.; Foresman, J. B.; Ortiz, J. V.; Cui, Q.; Baboul, A. G.; Clifford, S.; Cioslowski, J.; Stefanov, B. B.; Liu, G.; Liashenko, A.; Piskorz, P.; Komaromi, I.; Martin, R. L.; Fox, D. J.; Keith, T.; Al-Laham, M. A.; Peng, C. Y.; Nanayakkara, A.; Challacombe, M.; Gill, P. M. W.; Johnson, B.; Chen, W.; Wong, M. W.; Gonzalez, C.; Pople, J. A. Gaussian, Inc.: Wallingford, CT, 2004.
(19) Ehlers, A. W.; Bohme, M.; Dapprich, S.; Gobbi, A.; Hollwarth, A.; Jonas, V.; Kohler, K. F.; Stegmann, R.; Veldkamp, A.; Frenking, G. *Chem. Phys. Lett.* **1993**, *208*, 111.
(20) Hollwarth, A.; Bohme, M.; Dapprich, S.; Ehlers, A. W.; Gobbi, A.; Jonas, V.; Kohler, K. F.; Stegmann, R.; Veldkamp, A.; Frenking, G. *Chem. Phys. Lett.* **1993**, *208*, 237.
(21) Hehre, W. J.; Ditchfield, R.; Pople, J. A. *J. Chem. Phys.* **1972**, *56*, 2257.
(22) Rassolov, V. A.; Ratner, M. A.; Pople, J. A.; Redfern, P. C.; Curtiss, L. A. *J. Comput. Chem.* **2001**, *22*, 976.